Electronic Supplementary Material (ESI) for Journal of Materials Chemistry A.

Silsesquioxane-based thiophene-bridged hybrid nanoporous network as a highly efficient adsorbent for wastewater treatment

Mingtao Ge, and Hongzhi Liu*

Key Laboratory of Special Functional Aggregated Materials, Ministry of Education, School of Chemistry and Chemical Engineering, Shandong University, Jinan 250100, P. R. China

*Corresponding Author. Fax: +86 531 88364691, E-mail: liuhongzhi@sdu.edu.cn

Characterization

Fourier-transform infrared (FT-IR) spectra of the products were performed with a Bruker Tensor 27 spectrophotometer from 4000 to 400 cm^{-1} at a resolution of 4 cm^{-1} (KBr pellet). Solution-state ^{13}C NMR and ^{29}Si NMR spectra were recorded with a Bruker Avance 400 spectrometer in $CDCl_3$ with tetramethylsilane as the internal standard. The resonance frequencies were 100 MHz for ^{13}C NMR, and 80 MHz for ^{29}Si NMR spectroscopy. Solid-state ^{13}C cross-polarization/magic-angle-spinning(CP/MAS) NMR and ^{29}Si MAS NMR spectra were performed with a Bruker AVANCE-500 NMR Spectrometer operating at a magnetic field strength of 9.4 T. The resonance frequencies at this field strength were 125 and 99 MHz for ^{13}C NMR and ^{29}Si NMR, respectively. A chemagnetics 5 mm triple-resonance MAS probe was used to acquire ^{13}C NMR and ^{29}Si NMR spectra. ^{29}Si MAS NMR spectra with high power proton decoupling were recorded using a p/2 pulselength of 5 ms, a recycle delay of 120 s and a spinning rate of 5 kHz. Elemental analysis was conducted by using an Elementarvario EL III elemental analyzer. Thermogravimetric analyses (TGA) were measured on a MettlerToledoSDTA-854 TGA/DSC system under nitrogen (100 mL min^{-1}) at a heatingrate of 10 °C min^{-1}. Powder X-ray diffraction (PXRD) was investigated by using a Riguku D/MAX 2550 diffractometerunder Cu-Kα radiation, 40 kV, 200 mA with the 2-Theta range of 5 to 80° (scanning rate of 10° min^{-1}) at room temperature. Field-emission scanning electronmicroscopy (FE-SEM) experiments were performed by using a HITACHI S4800 spectrometer. The high-resolution transmission electron microscopy (HR-TEM) experiments were recorded on a JEM 2100 electron microscope (JEOL, Japan) with an acceleration voltage of 200 kV.

Nitrogen sorption isotherm measurements were recorded by using a Micro Meritics surface area and pore size analyzer. The samples were degassed at 160 ℃ for 12 h prior to measurement. A sample of ca. 0.1 g and a UHP-grade nitrogen (99.999%) gas source were selected in the nitrogen sorption measurements at 77 K and collected on a Quantachrome Quadrasorb apparatus BET surface areas were evaluated at a P/P_0 range of 0.01 to 0.20. Nonlocal density functional theory (NL-DFT) pore size distributions were performed on the carbon/slit-cylindrical pore mode of the Quadrawin software. Carbon dioxide (CO_2) adsorption isotherm was measured with aTriStar II 3020V1.04. Prior to the measurements, the sample was degassed at 150 ℃ for at least 10 h. The UV − vis absorption spectra were obtained by a TU-1901 double beam UV-vis spectrophotometer. The concentration of the heavy metal ions in the solution is detected by an Optima 7000 DV Inductively Coupled Plasma atomic Emission Spectrometer (ICP-AES) (Thermo Perkin-Elmer). The concentration of Hg^{2+} in simulated wastewater was detected by Atomic fluorescence spectrometer.

Adsorption experiments

The batch mode adsorption was carried out to investigate the adsorption kinetics and adsorption capacities for dyes, including Rhodamine B (RB), Methylene Blue (MB) and Methyl Orange(MO). Dye concentration was determined by measuring at the maximum absorption wavelength using a UV-vis spectrophotometer (554 nm for Rhodamine B, 664 nm for Methylene Blue, and 463 nm for methyl orange). Before adsorption test, the relationship between absorbance and concentration was established by using UV-vis spectrophotometer. In the process of dye removal, 5 mg of THPP was added to 30 ml of dye aqueous solution with different concentrations and the mixture was stirred at room temperature. The concentration of dye solutions before and after adsorption was determined by employing a UV/vis spectrophotometer. For high concentration dyes, dye samples were diluted before absorbance measurements. In the process of heavy metal ion adsorption, 5 mg of THPP was dispersed in 15 ml of heavy metal ion aqueous solution. The concentration of the heavy metal ions in the solution before and after adsorption was detected by inductively coupled plasma atomic emission spectrometer (ICP-AES). To achieve the equibrium adsorption isotherm, dye solutions and heavy metal ion solutions were stirred overnight.

The amount of adsorbate adsorbed at equilibrium q_e (mg/g) was calculated from the following equation.

$$q_e = \frac{(c_o - c_e)V}{m}$$

Where c_0 and c_e (mg/L) are the initial and equilibrium concentrations of solute,V (L) is the volume of solution, m (g) is the mass of dry adsorbent.

In the adsorption kinetic experiments, the adsorption capacity at time t (min) can be calculated using the following equation:

$$q_t = \frac{(c_0 - c_t)V}{m}$$

Where c_t is concentrations of dye at time t (min), c_0 (mg/L), V (L), and m (g) are mentioned above.

Removal efficiency can be calculated by the following equation.

$$\text{Removal efficiency (\%)} = \frac{c_0 - c_e}{c_0} \times 100$$

Table S1 Surface properties for THPP.

Polymer	$S_{BET}{}^{a}$(m^2 g^{-1})	$S_{Micro}{}^{b}$(m^2 g^{-1})	$V_{Micro}{}^{c}$($cm^3 g^{-1}$)	$V_{Total}{}^{d}$($cm^3 g^{-1}$)	V_{Micro}/V_{Total}
THPP	915	230	0.095	1.61	5.9%

[a] Surface area calculated from the N_2 isotherm. [b] Microporous surface area calculated from the N_2 adsorption isotherm using the t-plot method. [c] The micropore volume derived using the t-plot method. [d] Total pore volume calculated at P/P_0 = 0.99.

Table S2 Physical and chemical properties of dyes

Properties	RB	MB	MO
Chemical formula	$C_{28}H_{31}ClN_2O_3$	$C_{16}H_{18}ClN_3S$	$C_{14}H_{14}N_3SO_3Na$
Molecular weight	479.01(g/mol)	319.85 (g/mol)	327.33(g/mol)
Dye nature	Basic	Basic	Acidic
Molecular size(nm)	1.59 ×1.18 ×0.56	1.26× 0.77× 0.65	1.31×0.55×0.18
Molecular structure	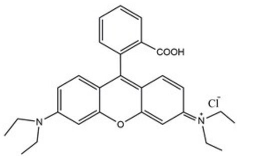	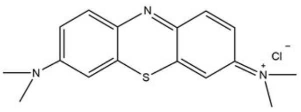	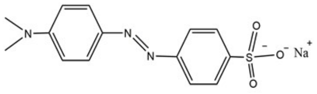

Table S3 Kinetic parameters for pseudo-second-order model and pseudo-first-order model.

			Pseudo-second-order model			Pseudo-first-order model		
adsorbate	C_0(mg/L)	$q_{e,exp}$(mg/g)	$q_{e,cal}$(mg/g)	k_2	R^2	$q_{e,cal}$(mg/g)	k_1	R^2
RB	158.9	884.4	917.4	0.00018	0.999	853.4	0.1040	0.8423
MB	51.3	262.4	261.1	0.0105	0.999	259.4	0.3196	0.8079
MO	44	105.9	115.6	0.00047	0.990	96.3	0.0546	0.7538

Table S4 Summary of the Langmuir and Freundlich isotherm model parameters for the adsorption of the heavy metal ions on THPP

	Langmuir			Freudlich		
adsorbate	q_m (mg g^{-1})	K_L	R^2	K_F	n	R^2
Ag^+	75.5	0.2646	0.9935	31.9673	4.7931	0.9786
Hg^{2+}	47.2	0.2921	0.9978	24.3709	6.5941	0.8359
Pb^{2+}	39.2	0.5398	0.9953	19.2775	4.9940	0.9774

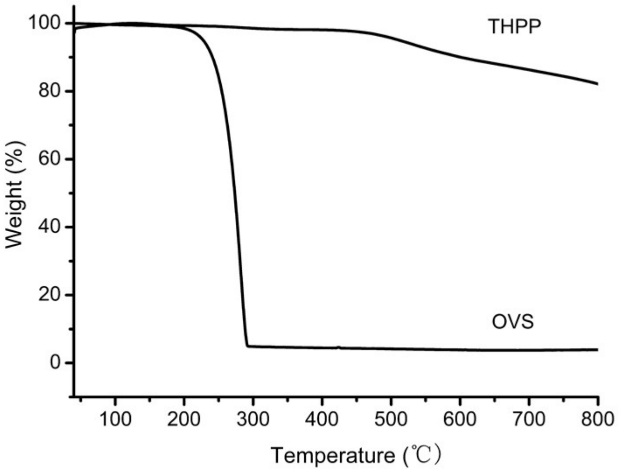

Figure S1. TGA curves of OVS and THPP.

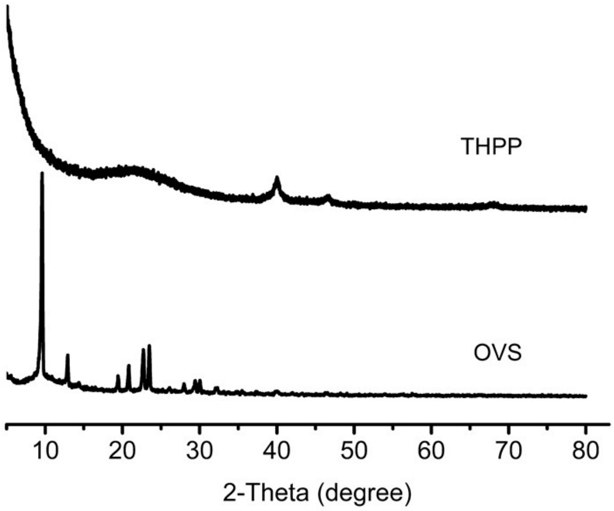

Figure S2. Powder XRD patterns of OVS and THPP.

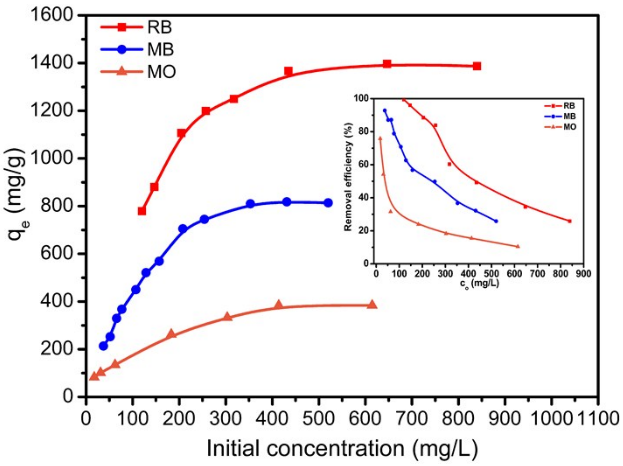

Figure S3. Effect of initial concentration on the adsorption of the dyes by THPP (inset is the effect of initial concentration on the removal efficiency).

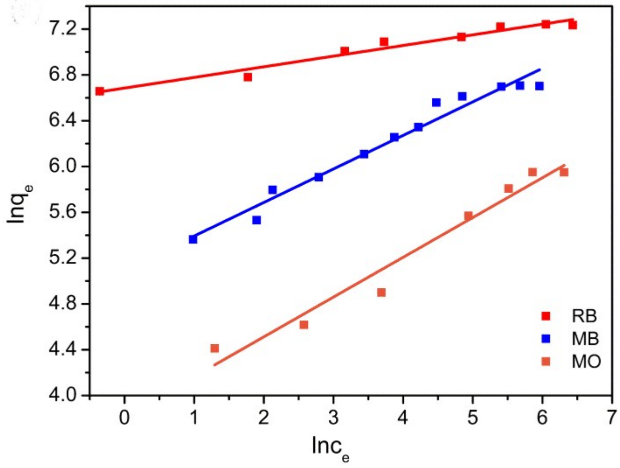

Figure S4. The linear regression of dyes adsorption by fitting the equilibrium adsorption data with Freundlich adsorption mode.

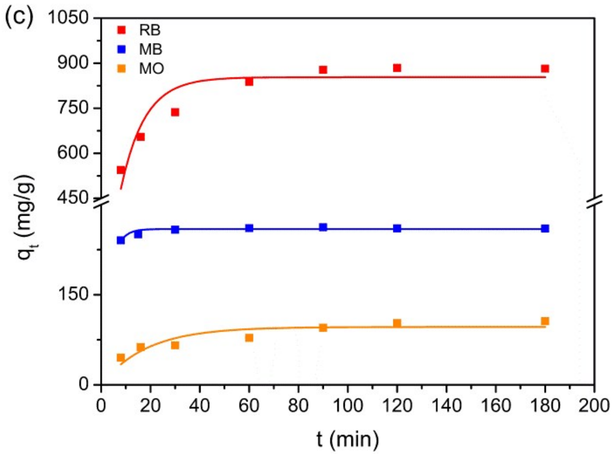

Figure S5. Pseudo-first-order kinetic plots for adsorption of dyes by THPP.

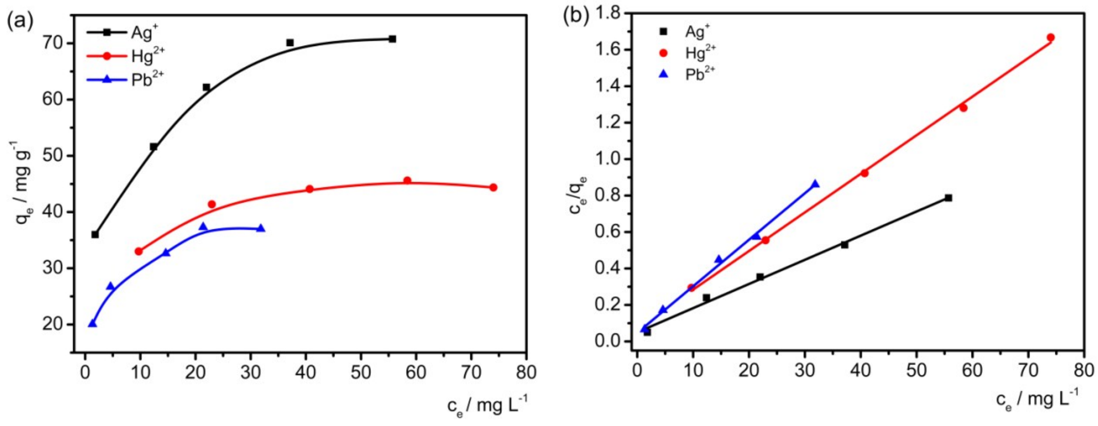

Figure S6. (a) Equilibrium adsorption isotherms of the heavy metal ions on THPP, (b) Shows the linear regression of the heavy metal ions adsorption by fitting the equilibrium adsorption data with Langmuir adsorption mode.

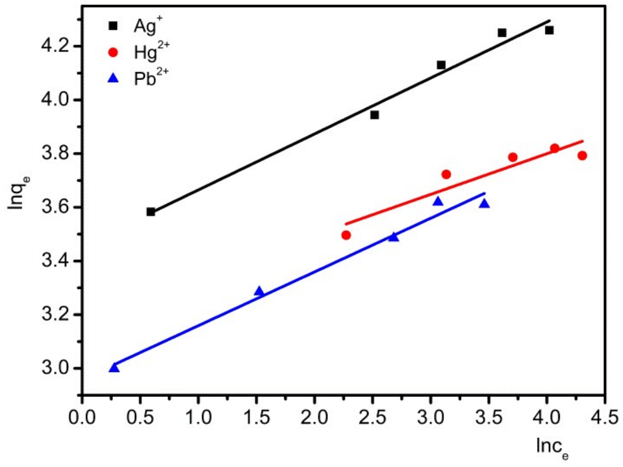

Figure S7. The linear regression of heavy metal ions adsorption by fitting the equilibrium adsorption data with Freundlich adsorption mode